Published in final edited form as:
Biochemistry. 2011 April 12; 50(14): 2769–2779. doi:10.1021/bi101161j.

Monoclonal Antibody m18 Paratope Leading to Dual Receptor Antagonism of HIV-1 gp120†

Syna Kuriakose Gift[‡,§], **Karyn McFadden**[‡], **Isaac J. Zentner**[‡], **Srivats Rajagopal**[‡], **Mei-Yun Zhang**[‖], **Dimiter S. Dimitrov**[⊥], and **Irwin M. Chaiken**[‡,§,*]

[‡]Department of Biochemistry and Molecular Biology, Drexel University College of Medicine, Philadelphia, Pennsylvania 19102

[§]Biochemistry Graduate Program, Drexel University College of Medicine

[‖]AIDS Institute; Department of Microbiology, The University of Hong Kong, Hong Kong

[⊥]Center for Cancer Research Nanobiology Program, CCR, NCI-Frederick, NIH, Frederick, Maryland 21702

Abstract

We sought to identify sequences in the monoclonal antibody m18 complementarity determining regions (CDRs) that are responsible for its interaction with HIV-1 gp120 and inhibition of the envelope receptor binding sites. In the accompanying paper, we reported that m18 inhibits CD4 binding through a non-activating mechanism that, at the same time, induces conformational effects leading to inhibition of the coreceptor site. Here, we sought to define the structural elements in m18 responsible for these actions. Direct binding and competition analyses using surface plasmon resonance showed that YU-2 gp120 binding is stabilized by a broad paratope of residues in the m18 CDRs. Additionally, several m18 residues were identified for which mutants retained high affinity for gp120, but had suppressed CD4 and 17b inhibition activities. A subset of these mutants did, however, neutralize HXBc2 viral infection. The results obtained in this work demonstrate that the combined m18 paratope contains subsets of residues that are differentially important for the binding and inhibition functions of the m18 neutralizing antibody. The data also add to prior observations that high affinity antibodies that do not inhibit monomeric gp120 receptor site interactions may still exhibit significant antiviral activity.

HIV-1 is one of the most genetically diverse pathogens described to date. Entry is initiated by the encounter of the envelope spike protein, gp120, with the host cell receptors. The most conserved regions of gp120, consisting of the CD4 and coreceptor binding sites, are attractive targets for neutralization. However, these regions within the viral spike are hidden from the immune system through glycosylation and conformational masking (1–5). In spite of these obstacles, a number of potent neutralizing antibodies specific to the envelope have been identified. Some potent antibodies to gp120 are b12 and VRC01, directed against the CD4 binding site (CD4bs), and 2G12, which recognizes a carbohydrate epitope on the outer domain (6–12). Antibodies which bind to the quaternary structure of the envelope, PG9 and PG16, bind to the V2 and V3 loops of gp120, but do not bind to gp120 alone (13, 14). They

†This research was supported by National Institute of Health grant P01 GM 56550 and CHAVI U19AI067854-04.

*To whom correspondence should be addressed. Drexel University College of Medicine, 11102 New College Building, MS 497, 245N 15th Street, Philadelphia PA 19102. Phone: 215-762-4197. Fax: 215-762-4452. ichaiken@drexelmed.edu.

SUPPORTING INFORMATION AVAILABLE

(1) Fab m18 mutant competition of YU-2 gp120 binding to immobilized CD4 and immobilized mAb 17b. This material is available free of charge via the internet at http://pubs.acs.org.

bind to an epitope formed by these loops on trimeric gp120 and also a carbohydrate epitope and represent new target sites by which to combat HIV-1 entry (13, 15–17). Recently, an additional neutralization site has been identified on gp120 proximal to the CD4bs and antibodies to this site, such as HJ16, make interactions with residues that do not overlap with those of other CD4bs antibodies (18, 19). The rarity of such gp120 neutralizing antibodies makes them important tools in studying vulnerable structural elements and possible inhibitory mechanisms.

Among the already-identified neutralizing antibodies against HIV-1 envelope gp120, two easily distinguishable classes are those to the CD4bs, such as b12, and those to the N-linked glycosylation sites, such as 2G12. 2G12 inhibits gp120 by binding to a glycosylation site on the outer domain, is thus not directly competitive for gp120 binding to CD4 or coreceptor, but nonetheless inhibits viral entry into the host cell (9, 10, 20–22). The inhibitory effect of 2G12 is thus primarily manifested by its impact on structure of envelope in the virus trimer spike. On the other hand, b12 binds to a site that overlaps with the CD4bs and at the same time disrupts this site by stabilizing a structure of gp120 monomer that is unique from the activated state (6, 8, 23). Furthermore, b12 induces conformational changes within the inner domain and bridging sheet that in effect disrupt the activated conformation of gp120 (23). F105, another CD4bs antibody, and also blocks the formation of the bridging sheet (24). While both of these CD4bs antibodies physically occlude the Phe43 cavity and entrap gp120 into a non-activated conformation, the structures of gp120 stabilized by these antibodies are different. Understanding these differences may help determine why b12 is so broadly neutralizing whereas F105 is not. Overall, what is common amongst these CD4bs antibodies is the blockade of CD4 binding and entrapment of the gp120 protein from a significantly disordered ground state into a functionally suppressed structure. As described in the preceding paper, the neutralizing mAb m18 has a mode of action that bears many similarities to CD4bs antibodies including induction of a functionally suppressed soluble gp120 monomer conformation.

M18 was isolated through phage display technology (25, 26). Mutational analysis revealed that the epitope for m18 binding is largely localized to the outer domain of gp120, overlapping the conserved b12 and CD4 epitopes (6, 27). The m18 complementarity determining region denoted as heavy chain three (HCDR3), composed largely of hydrophobic residues and forms a β-hairpin-like structure with a number of hydrogen bonds formed between residues within this loop, closely resembles the Phe43 binding loop of CD4. Docking models of Fab m18, along with mutational analysis on gp120, suggested that the HCDR3 loop of the antibody might be able to insert itself into the CD4 binding pocket of gp120, thereby blocking CD4 binding (27). However, in the accompanying paper, we reported that m18 does not mimic CD4.

In the work described here, we sought to define the structural elements within m18 that are critical for binding to HIV-1 gp120 and inhibition of receptor binding to gp120. We performed alanine scanning mutagenesis on the CDRs of Fab m18. We identified the YU-2 gp120 binding determinants through SPR analysis and further characterized the ability of these m18 mutants to inhibit gp120 interactions with soluble CD4 and IgG 17b. These studies revealed a broad paratope on m18 for gp120 binding. A small set of residues was also found to be critical for inhibition of CD4 and 17b binding, but not for m18 affinity to gp120. Several mutants of m18 with suppressed receptor binding inhibition still exhibited HXBc2 antiviral activity in cell infection assays. The ability to separate binding and inhibitory structural elements in m18 is consistent with a mode of function that is at least partly controlled by conformational effects on the envelope protein.

EXPERIMENTAL PROCEDURES

Reagents and Proteins

The HIV-1_{YU-2} gp120, HIV-1_{HXBc2} gp120, and HIV-1_{HXBc2} gp140 expression plasmids were kind gifts from Dr. Joseph Sodroski. CHO-ST4.2 cells were obtained through the AIDS Research and Reference Reagent Program, Division of AIDS, NIAID, NIH from Dr. Dan Littman. HOS-CD4-CXCR4 cells and pNL4-3.Luc.R-E- were obtained through the AIDS Research and Reference Reagent Program, Division of AIDS, NIAID, NIH from Dr. Nathaniel Landau. The monoclonal antibody, 17b, was purchased from Strategic Biosolutions, USA.

Gp120 Protein Expression and Purification

HIV-1_{YU-2} gp120 and HIV-1_{HXBc2} gp120 were in the expression vector pcDNA3.1 and were produced as soluble protein in mammalian cells using the 293F Invitrogen protocol. Briefly, a one liter culture volume of freestyle human embryonic kidney cells (HEK 293F) were grown to a density of one million cells/mL under 7.4% CO_2 in Gibco Freestyle 293F media (Invitrogen, CA). The cells were then transfected with 1 milligram of plasmid DNA per liter of culture using 293F Fectin (Invitrogen) and Opti-MEM I (Invitrogen, CA). The cells were grown at 37°C in 7.4% CO_2 for five days, after which the supernatant was clarified and the protein was purified. Both gp120s were purified via affinity chromatography through a column with the monoclonal antibody, 17b, immobilized onto Sepharose beads coated with Protein A to produce a homogeneous population of protein. The clarified supernatant containing the gp120s was passed through the column at 1 mL/minute to bind functional protein to the column. This was followed by repeated washings of the column with phosphate buffered saline solution (PBS; 0.01 M NaH_2PO_4, 0.15 M NaCl, pH 7.2), and then the bound gp120 was eluted using 0.1 M glycine, pH 2.5. The proteins were concentrated and exchanged into PBS and stored at −80°C.

Fab m18 Mutagenesis, Expression and Purification

The Fab m18 gene is contained in the phage display vector, pComb3x. Site-directed mutagenesis was performed using standardized techniques (Stratagene, CA) to create the various alanine mutations. The mutated DNA was verified by sequencing and then transformed into HB2151 cells (Maxim Biotech, CA). The transformed cells were grown in super broth media at 37°C until the optical density reached 0.8 absorption units. Protein expression was then induced with 2mM IPTG and grown at 30°C for 18 hours. Cells were spun down and resuspended in PBS with 20nM PMSF, 100μM lysozyme, and 100μM DNase VI. The cells were then sonicated at 50% power with repeated cycles of 15 seconds on and 10 seconds off for five minutes. The lysed cells were spun down at 18,000 rpm for 20 minutes and the supernatant was passed through a 0.2μm filter. Fab m18 and its mutants were affinity purified via protein G chromatography and eluted from the column with 0.1M glycine, pH 2.5. The proteins were exchanged into PBS and stored at −20°C.

Soluble CD4 Production

Soluble CD4 (sCD4) was produced from CHO-ST4.2 cells and contained all four extracellular domains of the receptor. The soluble protein was secreted by the cells into the supernatant and purified as described previously (28).

Surface Plasmon Resonance Binding Analysis

All surface plasmon resonance (SPR) assays were performed at 25°C on a BIAcore 3000 instrument (GE Healthcare, USA). Ligands were immobilized onto a CM5 dextran sensor surface through standard amine coupling techniques using 0.2 M EDC and 0.05 M NHS,

based on manufacturer protocols and as described previously (29). A reference surface was created through immobilization of IgG 2E3, an anti-IL5 monoclonal antibody and, along with PBS buffer injections, was used to correct for non-specific interactions and instrumental artifacts.

Direct binding interactions of m18 and its mutants to YU-2 and HXBc2 gp120 were studied through SPR. Gp120 (600 RU) was immobilized onto the surface of a CM5 chip. Serial dilutions of m18 and its mutants were made in PBS and injected over the gp120 surface at 50 μL/min with a 250 second association and up to 300 second dissociation. The 2E3 and gp120 surfaces were then regenerated with a five second pulse of 10 mM glycine, pH 1.5 at 100 μL/minute. Kinetic analysis of m18 binding to gp120 was performed by fitting the binding curves to a Langmuir 1:1 model using the BIAevaluation 4.0 program, with low residuals and Chi2. This analysis determined the average k_a and k_d values, which were then used to calculate the associated K_A and K_D values.

Competition assays were performed to study Fab m18 and mutant inhibition of YU-2 and HXBc-2 gp120 binding to sCD4 and 17b. For these experiments, sCD4 (2000 RU) and 17b (700 RU) were immobilized onto a sensor surface. The sCD4 surface was regenerated with a five second pulse of 1.3 M sodium chloride, 35 mM sodium hydroxide at 100 μL/minute. The 17b surface was regenerated with a five second pulse of 10 mM glycine, pH 1.5 at 100 μL/minute (29, 30). Increasing concentrations of m18 and m18 mutants (4 to 500 nM) were premixed with a final concentration of 100 nM gp120 and then passed over the sensor surface to detect gp120 binding to the immobilized sCD4 and 17b. Each concentration series was analyzed in sequence as a set, and then the analysis of the concentration series was repeated two more times, resulting in a total of 3 analyses per concentration. Premixed samples of gp120 and either m18 or m18 mutant were incubated at 4°C until injection into the SPR flow cell. All samples in each concentration series were set up at the same time, such that incubation times at 4°C for each concentration combination varied from a minimum of 10 minutes (sufficient for complete equilibration) to a maximum of 355 minutes. This variable-incubation protocol was found not to affect the degree of competition measured for any given concentration. This was concluded from the similarity of results from repeat analyses with different premixing times over the entire time course. Data from a three-repeat series for representative mutants are shown for YU-2 gp120 in Supplementary Figure 1. Using the affinity for each of the mutants to gp120, we calculated how much protein was needed to saturate 100nM gp120 to greater than 95% (31). The data were analyzed by plotting the maximum response at steady state against the concentration of m18 in the solution and then fitting to a four parameter equation through the BIAevaluation 4.0 program (28). This analysis calculated the half maximal binding (IC_{50}) value.

Preparation of Recombinant Luciferase Expressing Virus and Cell Infection Assays

Single round recombinant, luciferase-reporter viruses were produced in HEK293T cells using Fugene transfection reagent (Qiagen) according to the manufacturer's protocol. Cells were seeded in T75 flasks (approximately 3×10^6 cells per flask) and transfected the following day with 4 μg of plasmid encoding the envelope HIV-1_{HXBc2} together with 8 μg of the envelope-deficient pNL4-3-Fluc+env– provirus developed by N. Landau (32). Culture supernatants containing viral particles were collected 48–72 hours after transfection, clarified by centrifugation, filtered, aliquoted and stored at −80°C until use. For inhibition experiments, the viral stocks were first incubated with serial dilutions of the inhibitor at 37 °C for 30 minutes. The mixture was added to human osteosarcoma cells which stably express CD4 and CXCR4 (HOS.CD4.CXCR4) for 48–72 hours. The cells were then lysed with passive lysis buffer (Promega) followed by freeze-thaw cycles. Luciferase assays were performed using 1 mM D-luciferin salt (Anaspec) as substrate and detected on a 1450 Microbeta Liquid Scintillation and Luminescence Counter (Wallac and Jet). IC_{50} values

were estimated using non-linear regression analysis with Origin 7 (Origin Lab). All experiments were performed in triplicate and results were expressed as relative infection with respect to cell infected with virus in the absence of inhibitor (100% infected).

RESULTS

Mutagenic Analysis of the m18 CDRs to Define the Paratope for gp120 Binding

Mutational analysis was performed on significantly exposed residues of the Fab m18 CDRs, as determined by the crystal structure (27). These included HCDR1 N30, N31, Y32, and Y33; HCDR2 D53, S54, D56, T57, P61, S62, S64 and S65; HCDR3 H96, F99, I100, R100a and Y102; LCDR1 R24, Q27, D28, Q30 and K31; LCDR2 S52, T53 and S56; LCDR3 R93 and P95.

The effects of single alanine mutations for each of the above residues on m18 binding to YU-2 gp120 were evaluated by interaction kinetics using SPR. We found that a large proportion of these single-site mutants had affinities which were reduced by an order of magnitude or more (Table 1). From the values of association (k_a) and dissociation (k_d) rates determined by SPR (Figure 1), mutants that led to a significant affinity loss were generally characterized by a substantially faster off rate rather than a slower on rate. The significant affinity loss in a large subset of single site mutants and the lack of specific sites of extreme mutational sensitivity argue that the YU-2 gp120 utilizes a broad binding surface on m18, encompassing multiple CDRs (Figure 2).

Impact of m18 Mutations on YU-2 gp120 Receptor Site Inhibition

We evaluated the ability of the Fab m18 mutants to inhibit sCD4 and IgG 17b binding to gp120 and the ligand inhibition data, expressed as IC_{50} values, are given in Table 1 for all of the mutants. We found that a majority of the m18 mutants which had a relatively large reduction in affinity also failed to have any observable inhibitory effects in the inhibition analysis performed through SPR. This analysis was constrained by a narrow window for observing inhibition potency due to the limiting amounts of proteins available for these studies. Although all the competition analyses did reach greater than 95% saturation for each of the m18 mutants tested, we could not test higher concentrations. The one exception was Y33A, which exhibited a reduced affinity for YU-2 gp120, but maintained its inhibitory effects. This behavior could be related to the fast on-rate observed for this mutant binding to YU-2 gp120.

In the case of m18 mutants with close to normal YU-2 gp120 affinities, we were struck by the presence of two types of behavior. A number of the mutants had a high affinity for YU-2 gp120, with K_D values within five-fold of the wild type, and maintained their inhibitor effects as expected. These mutants include Y32A and T57A of the heavy chain and Q27A, D28A, Q30A and R93A of the light chain. On the other hand, a subset of mutants that had high affinity for YU-2 gp120 showed significantly suppressed inhibition of YU-2 gp120 interactions with sCD4 and 17b. These mutants include D53A, H96A, F99A, I100A and R100aA of the heavy chain and K31A and S52A of the light chain. The distribution of residues for which mutations lead to high affinity binding to gp120 and reduced receptor inhibitory activity are depicted in Figure 4. The presence of such residues argues that gp120 binding and the suppression of receptor interactions are separable.

The observation of high affinity m18 mutants with suppressed inhibition suggests the possibility that three-component complexes might form. A potential caveat in SPR competition analyses is that complexes preformed between YU-2 gp120 and m18 mutants might dissociate during the course of the injection and the free YU-2 gp120 could bind to the immobilized ligand. That this is not likely is shown by the comparison of two mutants,

T57A and F99A in Figure 5A and 5B. Both of these mutants have similar off rates when binding to YU-2 gp120, yet their effects on receptor binding are starkly different as shown by the inhibitory action of T57A and the lack of inhibition by F99A. This suggests that pre-dissociation is not likely to explain the lack of inhibition seen in the SPR analysis. We carried out a follow-up SPR analysis to determine if direct binding could be detected between YU-2 gp120-F99A and immobilized CD4. As shown by the dose response analysis in Figure 5C, experimentally significant and dose dependent binding could be observed, though only at relatively high concentrations of YU-2 gp120 where F99A was saturating. The concentration dependence of the YU-2 gp120-F99A complex binding to immobilized CD4 suggests that the three component complexes can form, given the high soluble analyte concentrations used. CD4 and 17b competition of YU-2 gp120 binding to F99A, the reverse of the experiment depicted in Figure 5A and 5B, show that these ligands can compete with and block gp120 binding to F99A similar to the results published with wild type m18 in the accompanying paper. CD4 inhibited F99A binding with an IC_{50} value of 39 nM (±10) and 17b suppressed binding down to 20%.

Since the alanine replacements typically introduce large scale changes in the amino acid side chains, we examined the role of these side chains by introducing more conserved replacements. In several cases, including Y33F and K31R, these mutations actually led to a more severe loss of function than observed with the alanine replacement. Such results argue a critical role for the original side chain in m18 function. On the other hand, replacement of the heavy chain F99 with a tyrosine yielded a higher affinity mutant with significant receptor site binding suppression than with the alanine mutant, indicating that the functionally important feature for this residue's inhibitory function is an aromatic side chain.

Differential Effects of m18 Mutations on Inhibition of Monomeric HXBc2 gp120 versus Viral Envelope

Prior work by Zhang et al, 2003 (25) detected Fab m18 neutralization of HIV-1 viruses from a number of clades. Since we observed residues that bind well to YU-2 gp120 but with suppressed receptor binding inhibition, we evaluated how these mutants would be able to inhibit the envelope in the context of the virus spike. Fab m18 did not neutralize HIV-1_{YU-2} pseudotyped viruses in our cell infection assays, but neutralization did occur with HIV-1_{HXBc2}. Viral neutralization assays were performed with this lab-adapted strain of gp120, taken as a prototype example for the purposes of the current work, in order to understand the differences between wild-type m18 and a few of its mutant counterparts. We selected a panel of Fab m18 mutants, F99A, F99Y, I100A, K31A and S52A, along with wild type Fab m18 itself, and compared the mutational effects on the inhibition of monomeric HXBc2 gp120 interactions versus neutralization of the functional HXBc2 viral spike (Table 2). We first determined their binding and inhibitory properties against monomeric HXBc2 gp120 through SPR assays. As with YU-2 gp120, we identified mutants that retained strong binding for HXBc2 gp120, but had suppressed sCD4 and 17b binding inhibition (Figure 6). These included heavy chain I100A and light chain K31A and S52A. In contrast, both K31A and S52A were able to neutralize viral infection with nearly wild type efficacy. Interestingly, the mutant, F99A did not show any receptor inhibition for YU-2 gp120, but did show receptor inhibition for HXBc2 gp120 and was able to neutralize viral cell infection. The results with HXBc2 gp120 provide further support that m18 residues can function at distinguishable binding and ligand inhibition steps upon interaction. At the same time, the viral neutralization results demonstrate that m18 mutants can inhibit viral infection to an extent not predicted by their inhibition of monomeric HXBc2 gp120 receptor sites.

DISCUSSION

The HIV-1 interaction characteristics of mAb m18 argue that this antibody inhibits the viral envelope through a mechanism that involves conformational entrapment of the envelope protein into a functionally suppressed state (Gift et al, accompanying paper). While initial studies with YU-2 gp120 mutants showed that the m18 binding site is primarily localized to the outer domain of the envelope protein (27), the way m18 engages YU-2 gp120 is not the same as CD4. In the current study, we sought to deepen our understanding of how m18 binds and inhibits YU-2 and HXBc2 gp120 by evaluating site-directed mutants of this antibody.

We focused on residues of the m18 CDRs with solvent exposed side chains in order to minimize structural effects on m18 due to the mutation. Residues with a side chain exposure of 50% or greater were replaced by alanine residues in order to map residues important for interactions with YU-2 gp120 with minimal involvement in intramolecular interactions within m18 itself. The mutagenic analysis of the exposed residues showed that mutations affecting YU-2 gp120 binding are broadly distributed across the surface of the CDRs. Furthermore, none of the mutants had affinities that were reduced by more than 50-fold. This would indicate that m18 binding to YU-2 gp120 is stabilized by small contributions in energy from a large number of side chains versus a few residues with large contributions. Among other aspects, the YU-2 gp120 binding paratope is not dominated by the HCDR3 loop, which has a structure reminiscent of the Phe43 loop of CD4 (27). The mutagenic results argue that m18 engages YU-2 gp120 in a manner which is distinct from CD4. This is perhaps not surprising considering the dual receptor site antagonism exhibited by m18, compared to the activation of the YU-2 gp120 coreceptor binding site by CD4.

The mutagenic studies reported here were carried out in the absence of a high resolution structure of a gp120-m18 complex. Hence, a caveat of the work is that, while the role of residues in binding energetics can be defined, direct physical contact between the m18 paratope and the gp120 structure can only be inferred. In the case of b12, mutational effects tracked by ELISA defined residues in HCDR2, HCDR3 and LCDR1 as important for gp120 binding (8, 33). In contrast, the crystallographic structure localized the interface mainly on HCDR1, HCDR2 and HCDR3 (23). The b12 results highlight the complementarity of mutagenic and crystallographic data for defining antibody interactions of a protein system, such as gp120, that undergoes large conformational changes as part of the complexation process.

A second potential caveat of the current work is the possibility that mutations can have an effect on global structural stability as opposed to direct antibody contacts. This seems unlikely for the mutations reported here, all of which were expressed at high levels and involve residues in exposed regions with minimal intramolecular packing contacts. Mutations for which low expression was observed in this work were excluded in view of possible global destabilization in those cases.

Several mutants of m18 exhibited unexpectedly suppressed dual antagonist properties. While mutants with suppressed YU-2 gp120 affinity exhibited corresponding reduced inhibition of CD4 and 17b interactions, a subset of mutants with high affinity also showed reduced inhibition. These results suggest that m18 can bind to a site on gp120 that does not completely overlap the receptor sites. This is consistent with a two-step model of gp120-m18 interaction with an initial binding step and a secondary locking of the envelope protein into a functionally suppressed form. In this model, a subset of residues would be expected to allow gp120 binding but not the subsequent entrapment into a form with a suppressed receptor binding site. The conformational constraint of gp120 into an inactive conformation

by m18 is consistent with partial structuring of YU-2 gp120 seen through calorimetry (Gift et al, accompanying paper).

The finding of mutants that bind strongly to YU-2 gp120 but don't inhibit CD4 and 17b predict that three-component complexes should be able to form. We tested this possibility using the F99A mutant. Indeed, SPR analysis showed that YU-2 gp120 saturated with F99A bound to immobilized CD4 with an observably weak affinity of 0.71 μM (±0.04). Moreover, this interaction is directly affected by the orientation of the experiment. When CD4 is premixed with YU-2 gp120 first, gp120 binding to F99A is inhibited in a similar manner as wild type m18 (shown in the accompanying paper). It is likely that the three-component complex, observable kinetically in Figure 5C, is not stable at equilibrium. Indeed attempts during this study to observe three-component complexes in mixtures of F99A, YU-2 gp120 and CD4 by analytical ultracentrifugation failed to convincingly separate out such complexes. This could be due in part to the slower off rate of CD4, in comparison to F99A, preventing the formation of a long-lasting three-component complex of these two protein ligands with YU-2 gp120.

Wild type m18 has a high affinity for YU-2 and HXBc2 gp120, inhibits their receptor sites in SPR assays and suppresses recombinant HXBc2 viral infection. A number of m18 mutants that had high affinity for HXBc2 gp120 binding, but exhibited reduced or undetectable CD4 and 17b inhibition effects in SPR assays, were nonetheless found to suppress recombinant viral infection. This result is reminiscent of observations of significant anti-FLAG induced viral neutralization of pseudoviruses containing the FLAG sequence imported into the V4 loop of gp120. V4 is highly variable and distant from the binding sites for both CD4 and coreceptor. Antibodies directed at this inserted linear FLAG sequence were sufficient to reduce cell infection by the modified pseudotyped envelope by a maximum of 80%. The finding of residual (20%) infection even at saturating anti-FLAG was interpreted to indicate that the CD4 and coreceptor binding sites are not directly blocked by anti-FLAG binding to gp120 (34–36). Instead, the FLAG antibody results argued that non-competitive effects of an antibody on the functional virus spike could be sufficient to allow neutralization of the virus. The neutralization of HIV-1 HXBc2 pseudovirus by m18 mutants that do not inhibit CD4 and 17b interactions with monomeric HXBc2 and YU-2 gp120 appear analogous to the prior finding with anti-FLAG neutralization. Although these two strains of HIV-1 utilize different coreceptors (YU-2 utilizes CCR5 and HXBc2 utilizes CXCR4) during infection (37, 38), we have shown using gp120 mutants that m18 binding is independent of the coreceptor site (accompanying paper). Hence, we would expect that m18 inhibition should be independent of coreceptor usage. Furthermore, coreceptor usage is determined by the variable loops of gp120 (39), and we and others have shown that Fab m18 binds with high affinity to core gp120, which has all of the variable loops removed (23, 24). We cannot rule out the possibility that such mutants may inhibit receptor binding to YU-2 and HXBc2 gp120 in the context of trimeric envelope spike. We also cannot distinguish at present whether the non-inhibitory m18 mutants are neutralizing by altering envelope spike conformation or instead limiting receptor access to the receptor binding sites of the envelope spike. These HXBc2 viral neutralization assays were performed with a limited subset of Fab m18 mutants, representing the different patterns of competition observed through SPR, in order to identify the extent of the relationship between SPR and antiviral effects. The results obtained demonstrate that inhibition of monomeric HXBc2 gp120 receptor binding is not necessarily a predictor of antiviral cell infection effects.

Investigation of neutralizing antibodies against HIV-1 gp120 such as m18 can help determine how ligand interactions can lead to specific neutralization of the virus. Our results, taken in the context of other neutralizing antibodies, reveal that antagonizing viral entry may occur through different mechanisms of binding site inhibition and viral spike

disruption (3, 6, 13, 17, 18, 23, 24, 40–42). Understanding these different mechanisms may prove useful in determining productive routes to inhibit HIV entry.

Supplementary Material

Refer to Web version on PubMed Central for supplementary material.

Acknowledgments

This research was supported by the National Institute of Health grant P01 GM 56550 and by the Intramural Research Program of the NIH, National Cancer Institute, Center for Cancer Research. We are grateful to Dr. Joseph Sodroski for providing us with the DNA construct for full length gp120. We also thank Dr. Bradford Jameson, Dr. Patrick Loll, Dr. Fred Krebs, Dr. James Hoxie, Dr. Simon Cocklin and Dr. Ponraj Prabakaran for helpful discussions.

Abbreviations

AIDS	acquired immune deficiency syndrome
HIV-1	human immunodeficiency virus type 1
sCD4	soluble CD4
gp120	120 kDa glycoprotein
mAb	monoclonal antibody
CDR	complementarity determining region
PBS	phosphate–buffered saline
SPR	surface plasmon resonance

References

1. Yuan W, Bazick J, Sodroski J. Characterization of the multiple conformational States of free monomeric and trimeric human immunodeficiency virus envelope glycoproteins after fixation by cross-linker. J Virol. 2006; 80:6725–6737. [PubMed: 16809278]
2. Rizzuto CD, Wyatt R, Hernandez-Ramos N, Sun Y, Kwong PD, Hendrickson WA, Sodroski J. A conserved HIV gp120 glycoprotein structure involved in chemokine receptor binding. Science. 1998; 280:1949–1953. [PubMed: 9632396]
3. Kwong PD, Wyatt R, Robinson J, Sweet RW, Sodroski J, Hendrickson WA. Structure of an HIV gp120 envelope glycoprotein in complex with the CD4 receptor and a neutralizing human antibody. Nature. 1998; 393:648–659. [PubMed: 9641677]
4. Chen B, Vogan EM, Gong H, Skehel JJ, Wiley DC, Harrison SC. Structure of an unliganded simian immunodeficiency virus gp120 core. Nature. 2005; 433:834–841. [PubMed: 15729334]
5. Wyatt R, Kwong PD, Desjardins E, Sweet RW, Robinson J, Hendrickson WA, Sodroski JG. The antigenic structure of the HIV gp120 envelope glycoprotein. Nature. 1998; 393:705–711. [PubMed: 9641684]
6. Pantophlet R, Ollmann Saphire E, Poignard P, Parren PW, Wilson IA, Burton DR. Fine mapping of the interaction of neutralizing and nonneutralizing monoclonal antibodies with the CD4 binding site of human immunodeficiency virus type 1 gp120. J Virol. 2003; 77:642–658. [PubMed: 12477867]
7. Roben P, Moore JP, Thali M, Sodroski J, Barbas CF 3rd, Burton DR. Recognition properties of a panel of human recombinant Fab fragments to the CD4 binding site of gp120 that show differing abilities to neutralize human immunodeficiency virus type 1. J Virol. 1994; 68:4821–4828. [PubMed: 7518527]
8. Saphire EO, Parren PW, Pantophlet R, Zwick MB, Morris GM, Rudd PM, Dwek RA, Stanfield RL, Burton DR, Wilson IA. Crystal structure of a neutralizing human IGG against HIV-1: a template for vaccine design. Science. 2001; 293:1155–1159. [PubMed: 11498595]

9. Sanders RW, Venturi M, Schiffner L, Kalyanaraman R, Katinger H, Lloyd KO, Kwong PD, Moore JP. The mannose-dependent epitope for neutralizing antibody 2G12 on human immunodeficiency virus type 1 glycoprotein gp120. J Virol. 2002; 76:7293–7305. [PubMed: 12072528]
10. Scanlan CN, Pantophlet R, Wormald MR, Ollmann Saphire E, Stanfield R, Wilson IA, Katinger H, Dwek RA, Rudd PM, Burton DR. The broadly neutralizing anti-human immunodeficiency virus type 1 antibody 2G12 recognizes a cluster of alpha1-->2 mannose residues on the outer face of gp120. J Virol. 2002; 76:7306–7321. [PubMed: 12072529]
11. Wu X, Yang ZY, Li Y, Hogerkorp CM, Schief WR, Seaman MS, Zhou T, Schmidt SD, Wu L, Xu L, Longo NS, McKee K, O'Dell S, Louder MK, Wycuff DL, Feng Y, Nason M, Doria-Rose N, Connors M, Kwong PD, Roederer M, Wyatt RT, Nabel GJ, Mascola JR. Rational design of envelope identifies broadly neutralizing human monoclonal antibodies to HIV-1. Science. 2010; 329:856–861. [PubMed: 20616233]
12. Zhou T, Georgiev I, Wu X, Yang ZY, Dai K, Finzi A, Kwon YD, Scheid JF, Shi W, Xu L, Yang Y, Zhu J, Nussenzweig MC, Sodroski J, Shapiro L, Nabel GJ, Mascola JR, Kwong PD. Structural basis for broad and potent neutralization of HIV-1 by antibody VRC01. Science. 2010; 329:811–817. [PubMed: 20616231]
13. Walker LM, Phogat SK, Chan-Hui PY, Wagner D, Phung P, Goss JL, Wrin T, Simek MD, Fling S, Mitcham JL, Lehrman JK, Priddy FH, Olsen OA, Frey SM, Hammond PW, Kaminsky S, Zamb T, Moyle M, Koff WC, Poignard P, Burton DR. Broad and potent neutralizing antibodies from an African donor reveal a new HIV-1 vaccine target. Science. 2009; 326:285–289. [PubMed: 19729618]
14. Gorny MK, Stamatatos L, Volsky B, Revesz K, Williams C, Wang XH, Cohen S, Staudinger R, Zolla-Pazner S. Identification of a new quaternary neutralizing epitope on human immunodeficiency virus type 1 virus particles. J Virol. 2005; 79:5232–5237. [PubMed: 15795308]
15. Doores KJ, Burton DR. Variable loop glycan dependency of the broad and potent HIV-1-neutralizing antibodies PG9 and PG16. J Virol. 2010; 84:10510–10521. [PubMed: 20686044]
16. Zolla-Pazner S, Cardozo T. Structure-function relationships of HIV-1 envelope sequence-variable regions refocus vaccine design. Nat Rev Immunol. 2010; 10:527–535. [PubMed: 20577269]
17. Kwong PD, Wilson IA. HIV-1 and influenza antibodies: seeing antigens in new ways. Nature immunology. 2009; 10:573–578. [PubMed: 19448659]
18. Corti D, Langedijk JP, Hinz A, Seaman MS, Vanzetta F, Fernandez-Rodriguez BM, Silacci C, Pinna D, Jarrossay D, Balla-Jhagjhoorsingh S, Willems B, Zekveld MJ, Dreja H, O'Sullivan E, Pade C, Orkin C, Jeffs SA, Montefiori DC, Davis D, Weissenhorn W, McKnight A, Heeney JL, Sallusto F, Sattentau QJ, Weiss RA, Lanzavecchia A. Analysis of memory B cell responses and isolation of novel monoclonal antibodies with neutralizing breadth from HIV-1-infected individuals. PloS one. 2010; 5:e8805. [PubMed: 20098712]
19. Pietzsch J, Scheid JF, Mouquet H, Klein F, Seaman MS, Jankovic M, Corti D, Lanzavecchia A, Nussenzweig MC. Human anti-HIV-neutralizing antibodies frequently target a conserved epitope essential for viral fitness. J Exp Med. 2010; 207:1995–2002. [PubMed: 20679402]
20. Trkola A, Purtscher M, Muster T, Ballaun C, Buchacher A, Sullivan N, Srinivasan K, Sodroski J, Moore JP, Katinger H. Human monoclonal antibody 2G12 defines a distinctive neutralization epitope on the gp120 glycoprotein of human immunodeficiency virus type 1. J Virol. 1996; 70:1100–1108. [PubMed: 8551569]
21. Binley JM, Wrin T, Korber B, Zwick MB, Wang M, Chappey C, Stiegler G, Kunert R, Zolla-Pazner S, Katinger H, Petropoulos CJ, Burton DR. Comprehensive cross-clade neutralization analysis of a panel of anti-human immunodeficiency virus type 1 monoclonal antibodies. J Virol. 2004; 78:13232–13252. [PubMed: 15542675]
22. Binley JM, Ngo-Abdalla S, Moore P, Bobardt M, Chatterji U, Gallay P, Burton DR, Wilson IA, Elder JH, de Parseval A. Inhibition of HIV Env binding to cellular receptors by monoclonal antibody 2G12 as probed by Fc-tagged gp120. Retrovirology. 2006; 3:39. [PubMed: 16817962]
23. Zhou T, Xu L, Dey B, Hessell AJ, Van Ryk D, Xiang SH, Yang X, Zhang MY, Zwick MB, Arthos J, Burton DR, Dimitrov DS, Sodroski J, Wyatt R, Nabel GJ, Kwong PD. Structural definition of a conserved neutralization epitope on HIV-1 gp120. Nature. 2007; 445:732–737. [PubMed: 17301785]

24. Chen L, Do Kwon Y, Zhou T, Wu X, O'Dell S, Cavacini L, Hessell AJ, Pancera M, Tang M, Xu L, Yang ZY, Zhang MY, Arthos J, Burton DR, Dimitrov DS, Nabel GJ, Posner MR, Sodroski J, Wyatt R, Mascola JR, Kwong PD. Structural basis of immune evasion at the site of CD4 attachment on HIV-1 gp120. Science. 2009; 326:1123–1127. [PubMed: 19965434]
25. Zhang MY, Shu Y, Phogat S, Xiao X, Cham F, Bouma P, Choudhary A, Feng YR, Sanz I, Rybak S, Broder CC, Quinnan GV, Evans T, Dimitrov DS. Broadly cross-reactive HIV neutralizing human monoclonal antibody Fab selected by sequential antigen panning of a phage display library. J Immunol Methods. 2003; 283:17–25. [PubMed: 14659896]
26. Bessette PH, Rice JJ, Daugherty PS. Rapid isolation of high-affinity protein binding peptides using bacterial display. Protein Eng Des Sel. 2004; 17:731–739. [PubMed: 15531628]
27. Prabakaran P, Gan J, Wu YQ, Zhang MY, Dimitrov DS, Ji X. Structural mimicry of CD4 by a cross-reactive HIV-1 neutralizing antibody with CDR-H2 and H3 containing unique motifs. J Mol Biol. 2006; 357:82–99. [PubMed: 16426633]
28. McFadden K, Cocklin S, Gopi H, Baxter S, Ajith S, Mahmood N, Shattock R, Chaiken I. A recombinant allosteric lectin antagonist of HIV-1 envelope gp120 interactions. Proteins. 2007; 67:617–629. [PubMed: 17348010]
29. Dowd CS, Leavitt S, Babcock G, Godillot AP, Van Ryk D, Canziani GA, Sodroski J, Freire E, Chaiken IM. Beta-turn Phe in HIV-1 Env binding site of CD4 and CD4 mimetic miniprotein enhances Env binding affinity but is not required for activation of coreceptor/17b site. Biochemistry. 2002; 41:7038–7046. [PubMed: 12033937]
30. Biorn AC, Cocklin S, Madani N, Si Z, Ivanovic T, Samanen J, Van Ryk DI, Pantophlet R, Burton DR, Freire E, Sodroski J, Chaiken IM. Mode of action for linear peptide inhibitors of HIV-1 gp120 interactions. Biochemistry. 2004; 43:1928–1938. [PubMed: 14967033]
31. Schon A, Madani N, Klein JC, Hubicki A, Ng D, Yang X, Smith AB 3rd, Sodroski J, Freire E. Thermodynamics of Binding of a Low-Molecular-Weight CD4 Mimetic to HIV-1 gp120. Biochemistry. 2006; 45:10973–10980. [PubMed: 16953583]
32. Connor RI, Chen BK, Choe S, Landau NR. Vpr is required for efficient replication of human immunodeficiency virus type-1 in mononuclear phagocytes. Virology. 1995; 206:935–944. [PubMed: 7531918]
33. Zwick MB, Parren PW, Saphire EO, Church S, Wang M, Scott JK, Dawson PE, Wilson IA, Burton DR. Molecular features of the broadly neutralizing immunoglobulin G1 b12 required for recognition of human immunodeficiency virus type 1 gp120. J Virol. 2003; 77:5863–5876. [PubMed: 12719580]
34. Ren X, Sodroski J, Yang X. An unrelated monoclonal antibody neutralizes human immunodeficiency virus type 1 by binding to an artificial epitope engineered in a functionally neutral region of the viral envelope glycoproteins. J Virol. 2005; 79:5616–5624. [PubMed: 15827176]
35. Yang X, Kurteva S, Lee S, Sodroski J. Stoichiometry of antibody neutralization of human immunodeficiency virus type 1. J Virol. 2005; 79:3500–3508. [PubMed: 15731244]
36. Yang X, Lipchina I, Cocklin S, Chaiken I, Sodroski J. Antibody binding is a dominant determinant of the efficiency of human immunodeficiency virus type 1 neutralization. J Virol. 2006; 80:11404–11408. [PubMed: 16956933]
37. Doranz BJ, Orsini MJ, Turner JD, Hoffman TL, Berson JF, Hoxie JA, Peiper SC, Brass LF, Doms RW. Identification of CXCR4 domains that support coreceptor and chemokine receptor functions. J Virol. 1999; 73:2752–2761. [PubMed: 10074122]
38. Farzan M, Choe H, Vaca L, Martin K, Sun Y, Desjardins E, Ruffing N, Wu L, Wyatt R, Gerard N, Gerard C, Sodroski J. A tyrosine-rich region in the N terminus of CCR5 is important for human immunodeficiency virus type 1 entry and mediates an association between gp120 and CCR5. J Virol. 1998; 72:1160–1164. [PubMed: 9445013]
39. Pollakis G, Kang S, Kliphuis A, Chalaby MI, Goudsmit J, Paxton WA. N-linked glycosylation of the HIV type-1 gp120 envelope glycoprotein as a major determinant of CCR5 and CXCR4 coreceptor utilization. J Biol Chem. 2001; 276:13433–13441. [PubMed: 11278567]

40. Yang X, Kurteva S, Ren X, Lee S, Sodroski J. Stoichiometry of envelope glycoprotein trimers in the entry of human immunodeficiency virus type 1. J Virol. 2005; 79:12132–12147. [PubMed: 16160141]

41. Kwong PD, Wyatt R, Sattentau QJ, Sodroski J, Hendrickson WA. Oligomeric modeling and electrostatic analysis of the gp120 envelope glycoprotein of human immunodeficiency virus. J Virol. 2000; 74:1961–1972. [PubMed: 10644369]

42. Scheid JF, Mouquet H, Feldhahn N, Seaman MS, Velinzon K, Pietzsch J, Ott RG, Anthony RM, Zebroski H, Hurley A, Phogat A, Chakrabarti B, Li Y, Connors M, Pereyra F, Walker BD, Wardemann H, Ho D, Wyatt RT, Mascola JR, Ravetch JV, Nussenzweig MC. Broad diversity of neutralizing antibodies isolated from memory B cells in HIV-infected individuals. Nature. 2009; 458:636–640. [PubMed: 19287373]

43. Miller S, Janin J, Lesk AM, Chothia C. Interior and surface of monomeric proteins. J Mol Biol. 1987; 196:641–656. [PubMed: 3681970]

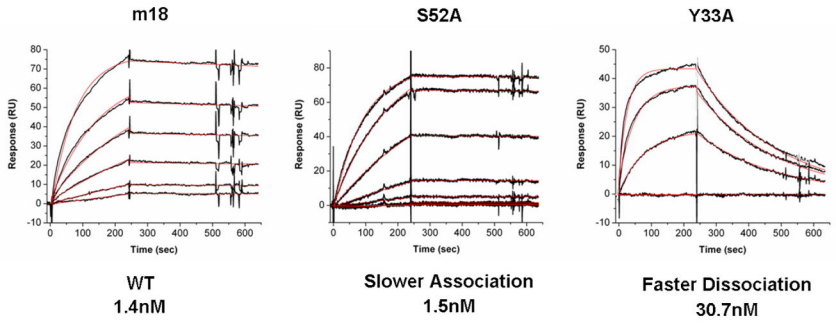

Figure 1.

Fab m18 and mutants binding to gp120. Fab m18 and its mutants at concentrations ranging from 4 to 500 nM were passed over a CM5 sensor surface which had immobilized YU-2 gp120 at a density of 600 RU. The direct binding sensorgrams were then fit to a Langmuir 1:1 binding model (red) using the BIAevaluation 4.0 program to calculate the affinity values and the data were plotted using Origin 7. These experiments were performed at least three times. On the left is wild type m18 with an affinity of 1.4 nM to YU-2 gp120. In the middle is the mutant, S52A. This mutant has a slower association rate than wild type (Table 1), but the calculated affinity comes out to be similar to wild type m18. On the right is the mutant, Y33A. This mutant has a faster dissociation rate, which is more obvious from the sensorgrams and the calculated affinity comes out to be 22 times weaker than wild type.

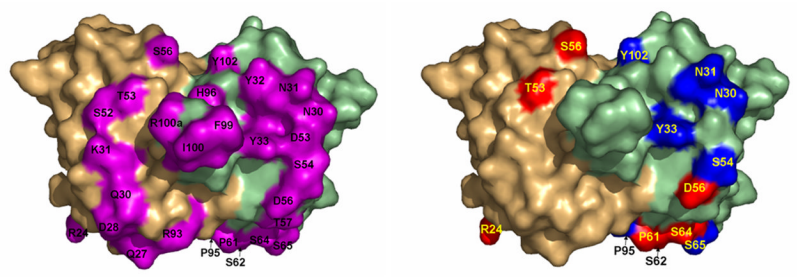

Figure 2.

Mutagenic Analysis of the M18 CDRs. Depicted here is the crystal structure of the Fab m18 CDRs with the protruding HCDR3 loop positioned at the center of the structure. The light chain is colored light orange and the heavy chain is colored green. The left figure depicts all the residues which were mutated to an alanine (magenta). The right figure depicts all the alanine mutants which had a 10 fold or greater decrease in affinity compared to wild type. Colored in blue are all the residues, when mutated to an alanine, had greater than 50% faster dissociation rate than wild type. In red are the alanine mutants which had both greater than 50% slower association and greater than 50% faster dissociation rate than wild type. The PDB code for this structure is 2AJ3 and was originally published by Prabakaran et al (27).

FIGURE 3A

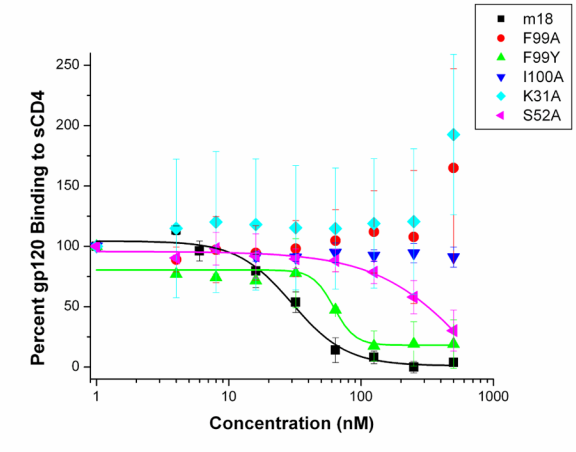

FIGURE 3B

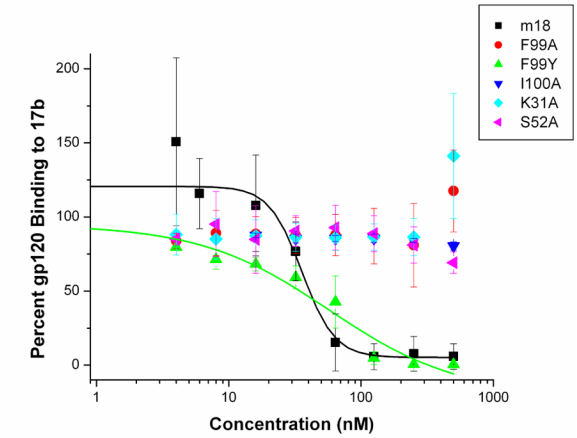

Figure 3.

Fab m18 and mutant competition of YU-2 gp120 binding to **(A)** sCD4 and **(B)** 17b. Fab m18 and its mutants, (■) m18, (●) F99A, (▲) F99Y, (▼) I100A, (♦) K31A and (◀) S52A, at concentrations ranging from 0 to 500 nM were premixed with 100 nM YU-2 gp120 before being passed over CM5 sensor surfaces which had immobilized sCD4 (A) and 17b (B). The maximum response at steady state for each concentration was fit to a four-parameter equation through the BIAevaluation program to determine the IC_{50} for inhibition of sCD4 and 17b binding to YU-2 gp120 and the average of three or more experiments are plotted through Origin 7. The data shown are in percent YU-2 gp120 binding to the sCD4 and 17b surfaces, respectively, and 100 nM YU-2 gp120, 0 nM Fab m18 represents 100% binding to the surface.

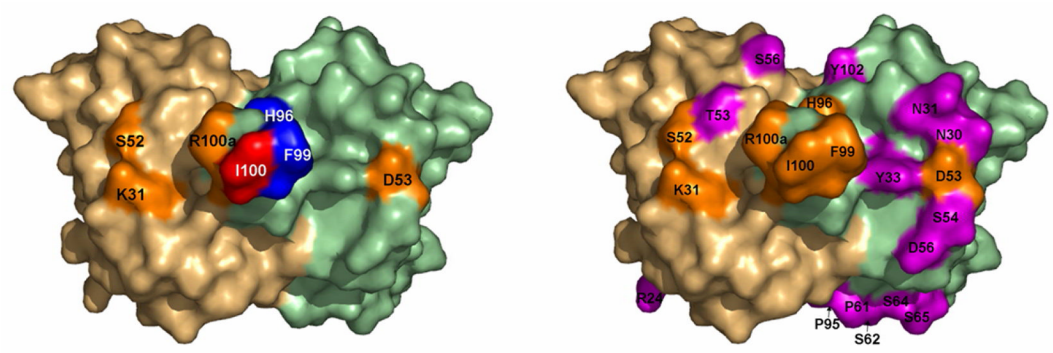

Figure 4.

High Affinity Mutants of M18. Depicted here is the crystal structure of the Fab m18 CDRs. The light chain is colored light orange and the heavy chain is colored green. The figure on the left highlights all the alanine mutants of m18 which retained high affinity binding to YU-2 gp120 (less than 10 fold loss in affinity compared to wild type m18), but lost all inhibitory activity against CD4 and 17b. Colored in blue are all the residues, when mutated to an alanine, had greater than 50% faster dissociation rate than wild type. Colored in orange are all the residues, when mutated to an alanine, had greater than 50% slower association rate than wild type. In red are the alanine mutants which had both greater than 50% slower association and greater than 50% faster dissociation rate than wild type. The figure on the right depicts residues important for binding to YU-2 gp120 in magenta and residues important for inhibition in orange. The PDB code for this structure is 2AJ3 and was originally published by Prabakaran et al (27).

FIGURE 5A

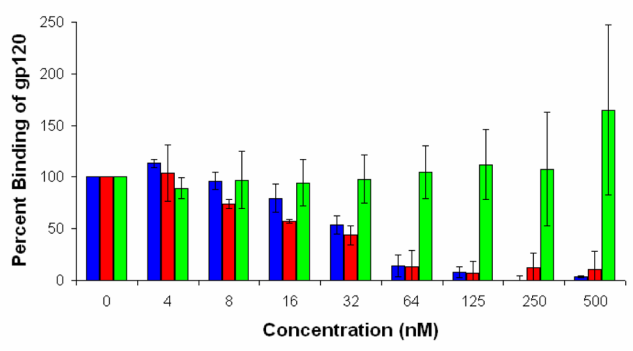

FIGURE 5B

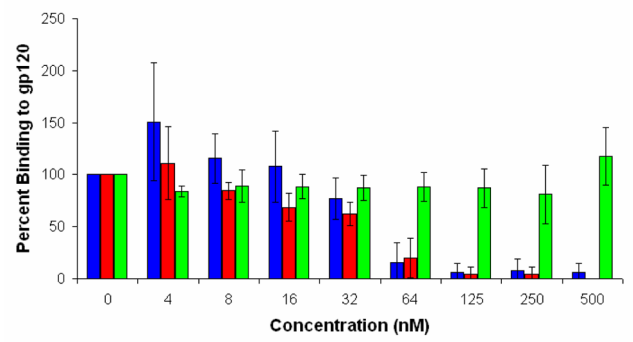

FIGURE 5C

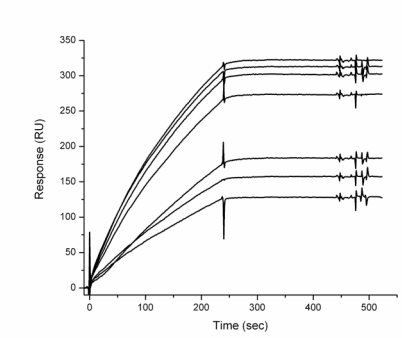

Figure 5.

Fab m18 and mutant competition. Increasing concentrations of Fab m18 (■), T57A (■) and F99A (■) were premixed with a fixed concentration of YU-2 gp120 (100nM) before being passed over immobilized **(A)** sCD4 and **(B)** 17b to detect competition. T57A and F99A have decreased stability in their dissociation rates, but opposite effects on the inhibition of sCD4 binding to gp120. The results of F99A competition in this analysis are similar to what was found for other similar mutants which are listed in Table 1. **(C)** Increasing concentrations of YU-2 gp120 (from 200 nM to 800 nM) were premixed with greater than 97% saturating levels of F99A (1uM) and passed over immobilized sCD4 to detect the formation of a potential three-component complex. The direct binding sensorgrams were then fit to a steady state affinity model using the BIAevaluation 4.0 program to calculate the affinity value (K_D = 0.7 ±0.04 μM). The data were plotted using Origin 7.

FIGURE 6A

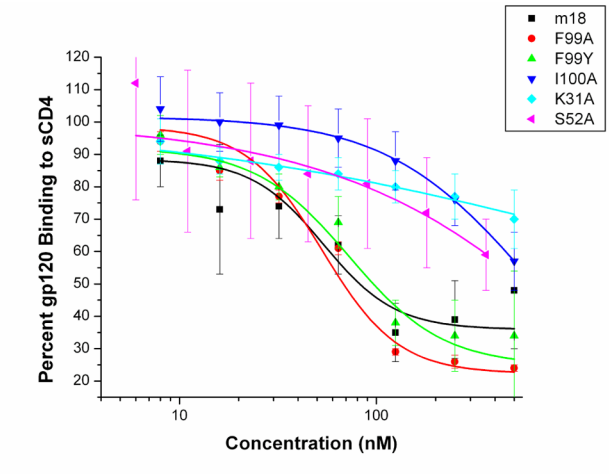

FIGURE 6B

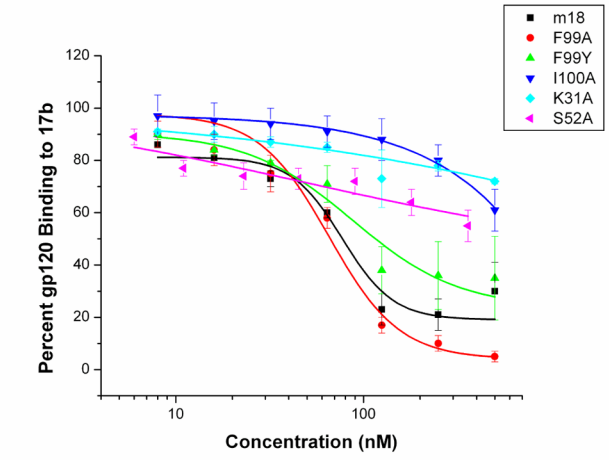

FIGURE 6C

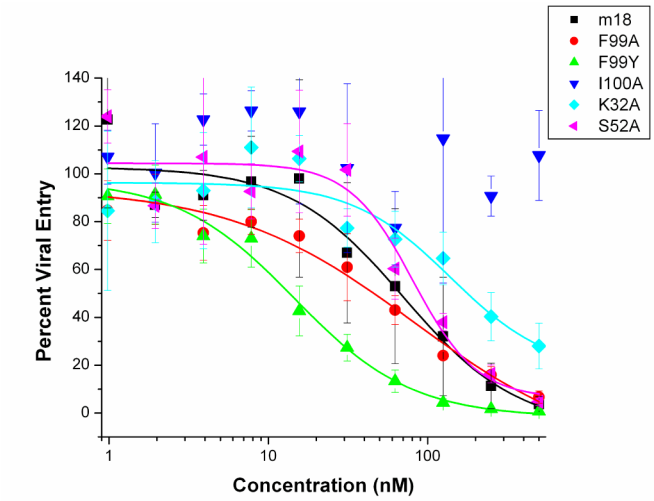

FIGURE 6D

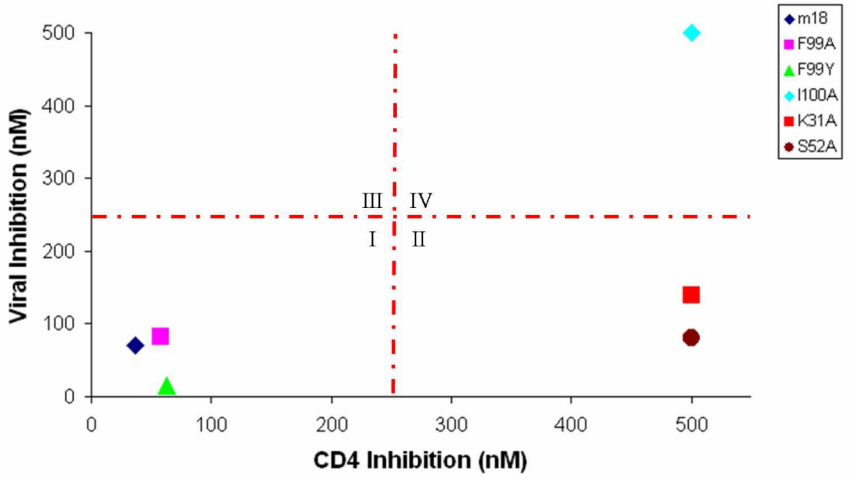

Figure 6.

Fab m18 and mutant competition of HXBc2 gp120 binding to **(A)** sCD4 and **(B)** 17b, and **(C)** viral inhibition with HXBc2 pseudotyped virus. Fab m18 and its mutants, (■) m18, (●) F99A, (▲) F99Y, (▼) I100A, (♦) K31A and (◀) S52A, at concentrations ranging from 0 to 500 nM were premixed with 100 nM HXBc2 gp120 before being passed over CM5 sensor surfaces which had immobilized **(A)** sCD4 and **(B)** 17b. The data shown are in percent gp120 binding to the sCD4 and 17b surfaces, respectively, and were fit in the same manner as Figure 2. **(C)** Recombinant single round, luciferase-reporter HIV-1_{HXBc2} viruses were incubated with increasing concentrations of m18 and mutants (0 to 500 nM) and then allowed to infect CD4 and CXCR4 positive cells. Infected cells were detected through luciferase assays and the IC_{50} values were estimated using non-linear regression analysis with Origin 7. **(D)** Comparison of competition of gp120 monomer binding and inhibition of pseudoviral cell infection by m18 mutants against monomeric and pseudotyped HXBc2 Env. The inhibition of sCD4 binding to HXBc2 gp120 by Fab m18 and five of its mutants is plotted against their ability to inhibit viral entry into cells. This is further divided into four theoretical quadrants. Fab m18 mutants in Quadrant I are those found to inhibit sCD4

binding to monomeric HXBc2 gp120 in solution assays, as well as to prevent viral cell entry. The mutant in Quadrant IV is ineffective in inhibiting both monomeric HXBc2 gp120 binding and viral cell infection. Mutants in Quadrant II are those that have suppressed inhibition of sCD4 binding to monomeric HXBc2 gp120, but are nonetheless effective in prevent viral entry into target cells. Mutants in Quadrant III (none found) would be effective in inhibiting sCD4, but ineffective at inhibiting viral entry. All experiments were performed in triplicate.

Table 1

Direct Binding Affinities and IC_{50} Values for Fab m18 Mutant Interactions with YU-2 Gp120 as Determined by SPR.[a]

Chain	Residue	Percent Side Chain Exposure*	k_a (1/Ms)	k_d (1/s)	K_D (nM)	% k_a	% 1/k_d	CD4 IC_{50} (nM)	17b IC_{50} (nM)
WT			6.9 e4 ± 0.3	9.8 e-5 ± 5.7	1.4	100	100	33.0 ± 3.6	36.0 ± 1.2
HCDR1	N30A	61	4.0 e4 ± 0.4	1.7 e-3 ± 0.3	40.9	58	6	>1000	>1000
	N31A	78	5.1 e4 ±1.0	1.3 e-3 ± 0.5	25.9	74	8	>1000	>1000
	Y32A	47	1.2 e5 ± 0.2	6.1 e-5 ± 3.0	0.4	217	161	247.3 ± 15.8	431.7 ± 31.5
	Y33A	45	1.2 e5 ± 0.5	3.8 e-3 ± 0.2	30.7	174	3	135.3 ± 7.1	149.7 ± 3.5
	Y33F		4.2 e4 ± 1.9	2.4 e-3 ± 0.8	56.3	61	4	>1000	>1000
HCDR2	D53A	47	1.6 e4 ± 1.3	1.2 e-4 ± 1.1	7.0	23	82	>500	>500
	S54A	48	3.9 e4 ± 0.5	2.2 e-3 ± 0.7	56.4	57	4	>1000	>1000
	D56A	74	2.5 e4 ± 0.6	6.1 e-4 ± 4.5	26.2	36	16	>1000	>1000
	T57A	68	8.4 e4 ± 2.0	2.1 e-4 ± 0.4	2.5	122	47	16.8 ± 3.8	33.1 ± 8.0
	P61A	61	3.3 e4 ± 1.0	6.3 e-4 ± 1.0	19.3	48	16	>1000	>1000
	S62A	45	3.5 e4 ± 0.9	1.6 e-3 ± 0.4	44.2	51	6	>1000	>1000
	S64A	62	2.1 e4 ± 0.7	8.6 e-4 ± 5.9	40.0	30	11	>1000	>1000
	S65A	80	3.6 e4 ± 1.2	1.4 e-3 ± 0.2	39.1	52	7	>1000	>1000
HCDR3	H96A	45	9.3 e4 ± 2.9	1.1 e-3 ± 0.6	11.7	135	9	>500	>500
	F99A	79	4.5 e4 ± 2.5	2.6 e-4 ± 1.5	5.9	65	38	>500	>500
	F99Y		9.4 e4 ± 2.5	1.1 e-4 ± 0.9	1.1	136	89	53.7 ± 1.5	75.3 ± 20.6
	I100A	71	2.7 e4 ± 1.3	3.6 e-4 ± 1.4	13.1	39	27	>500	>500
	R100AA	67	3.4 e4 ± 0.9	7.6 e-5 ± 5.1	2.3	49	129	>500	>500
	R100AE		1.6 e4 ± 0.6	1.1 e-3 ± 0.7	69.2	23	9	>1000	>1000
	Y102A	46	3.7 e4 ± 1.4	1.2 e-3 ± 0.4	31.5	54	8	>1000	>1000
LCDR1	R24A	79	2.3 e4 ± 0.9	3.9 e-4 ± 3.7	16.8	33	25	>1000	>1000
	Q27A	55	7.2 e4 ± 2.9	4.9 e-4 ± 3.9	6.7	104	20	49.6 ± 3.1	54.5 ± 3.5
	D28A	67	2.8 e4 ± 3.1	1.9 e-5 ± 0.7	0.7	41	516	65.5 ± 0.5	70.8 ± 1.8
	Q30A	43	9.1 e4 ± 0.1	1.2 e-4 ± 0.1	1.4	132	82	80.3 ± 16.7	129.3 ± 5.0
	K31A	58	2.9 e4 ± 0.4	8.9 e-5 ± 1.9	3.1	42	110	>500	>500

Chain	Residue	Percent Side Chain Exposure*	k_a (1/Ms)	k_d (1/s)	K_D (nM)	% k_a	% 1/k_d	CD4 IC_{50} (nM)	17b IC_{50} (nM)
	K31R		3.1 e4 ± 1.2	1.1 e-3 ± 0.2	34.7	45	9	>1000	>1000
LCDR2	S52A	51	1.7 e4 ± 0.9	8.1 e-5 ± 9.3	4.7	25	121	≥500	>500
	T53A	50	2.0 e4 ± 2.1	7.1 e-4 ± 7.0	35.2	29	14	>500	>500
	S56A	89	2.8 e4 ± 0.7	6.6 e-4 ± 1.4	25.7	41	15	>500	>500
LCDR3	R93A	46	3.9 e4 ± 0.2	8.0 e-5 ± 0.9	2.0	57	122	49.5 ± 20.5	78.7 ± 3.2
	P95A	44	5.3 e4 ± 1.6	1.9 e-3 ± 0.3	35.5	77	5	>1000	>1000

[a]Percent Side Chain Exposure was determined by analyzing the PDB structure of Fab m18 (2AJ3) through AREAIMOL1 to obtain the accessible surface areas for each atom by residue. The side chain atom accessibility was added up and a percentage was determined based on the total accessible surface area for amino acid side chains in a G – X – G peptide as determine by Miller et al (43).

Table 2

Direct Binding Affinities, SPR Based Competition, and Viral Inhibition Values for Fab m18 and Mutant Interactions with HXBc2 Gp120.

Chain	Residue	k_a (1/Ms)	k_d (1/s)	K_D (nM)	$\%k_a$	$\%1/k_d$	CD4 IC_{50} (nM)	17b IC_{50} (nM)	HxBC2 Viral Inhibition (nM)
WT		5.2 e4 ± 2.2	2.2 e-4 ± 0.9	4.3	100	100	36.1 ± 12.9	56.9 ± 13.0	70.8 ± 37.4
HCDR3	F99A	1.0 e5 ± 0.02	1.3 e-4 ± 0.1	1.3	192	169	58.2 ± 4.3	69.5 ± 3.7	81.8 ± 50.8
	F99Y	1.0 e5 ± 0.03	9.2 e-5 ± 0.6	0.9	192	239	62.8 ± 12.3	66.7 ± 6.1	14.6 ± 1.9
	I100A	1.7e4 ± 0.07	4.6 e-5 ± 1.0	2.8	33	478	>500	>500	>500
LCDR1	K31A	1.7e4 ± 0.5	3.1e-4 ±1.1	18.7	33	71	>500	>500	138.8 ± 106.5
LCDR2	S52A	3.5 e4 ± 2.1	2.0 e-5 ± 2.8	0.6	67	1100	>360	>360	81.0 ± 20.9